PHYSICAL REVIEW C **83**, 021601(R) (2011)

Systematics of reactions with ^{4,6}He: Static and dynamic halo effects and evidence for core-halo decoupling

E. F. Aguilera*
Departamento de Aceleradores, Instituto Nacional de Investigaciones Nucleares, Apartado Postal 18-1027, Código Postal 11801, México, Distrito Federal, México

I. Martel, A. M. Sánchez-Benítez, and L. Acosta
Departamento de Física Aplicada, Universidad de Huelva, E-21071 Huelva, Spain
(Received 24 December 2010; revised manuscript received 28 January 2011; published 28 February 2011)

Experimental reaction cross sections for ^{6}He and ^{4}He projectiles are reduced and are shown to follow well-defined trajectories that can be characterized by respective Wong-type curves. The strong enhancement observed for the ^{6}He data is interpreted as caused by two separate halo effects: a size effect, which affects the whole energy region, and a dynamic effect, important only near and below the barrier. Evidence for a core-halo decoupling is presented for the ^{6}He + ^{64}Zn system, which further supports the hypothesis that the decoupling is a characteristic feature of true halo systems.

DOI: 10.1103/PhysRevC.83.021601 PACS number(s): 25.60.Bx, 25.60.Dz, 21.10.Gv

Recently, it was shown that total reaction cross sections for ^{6}He (neutron halo) and ^{8}B (proton halo) with different targets, lie on the same trajectory when plotted in reduced form [1,2]. The scaling functions $\eta = (A_p^{1/3} + A_t^{1/3})^2$ and $\xi = Z_p Z_t/(A_p^{1/3} + A_t^{1/3})$ were used to reduce σ and $E_{\rm c.m.}$, respectively. A similar behavior is apparent for reactions with weakly bound but otherwise normal projectiles and also for strongly bound nuclei, but the two respective trajectories lie progressively lower in the plot with increasing binding energy of the projectile. The halo systems analyzed covered the energy range $0.6 \leqslant E_{\rm Red} \leqslant 2$, but it was noticed that, to ensure the accuracy of the obtained parametrization, it would be necessary to extend the analysis to other targets and energies, especially energies further above the barrier.

In a related work, it was shown that the experimental reaction cross sections for both ^{8}B + ^{58}Ni [1] and ^{6}He + ^{209}Bi [3] could be entirely accounted for by interactions of the halo state plus reactions that occur with the respective core. This led to the conclusion that a core-halo decoupling is present in both proton-halo and neutron-halo systems. In addition, the fact that the core and the valence neutron in the nonhalo nucleus ^{17}O behave differently [3], further supports the hypothesis that such a decoupling is actually a characteristic feature of true halo systems. Under this assumption, one may expect that the decoupling should show up in interactions of one single halo nucleus with different targets.

Within this context, the purpose of this Rapid Communication is to focus on reactions with ^{6}He, which is probably the best-studied neutron-halo nucleus. In an attempt to elucidate the specific effects of the halo, a comparison with reactions of the respective core, ^{4}He, will be performed.

As the first step, the systematics of interaction barriers of Ref. [2] will be extended. The idea is to include data for additional systems with energies that may cover an enlarged reduced-energy range. In addition to ^{209}Bi [4–6], reactions of ^{6}He with targets of ^{208}Pb [7], ^{197}Au [8], ^{120}Sn [9], ^{65}Cu [10], ^{64}Zn [11,12], ^{58}Ni [13], ^{27}Al [14], and ^{12}C [15–17] have been measured. Figure 1 includes reported results for these reactions, which adds quite a few experimental points to the ones presented for ^{6}He in Ref. [2]. Most of the additional points fall in the reduced-energy range previously analyzed, but the upper limit is actually extended up to $E_{\rm Red} \sim 4$.

For parametrization purposes, it is convenient to write Wong's formula [18] in terms of reduced quantities,

$$\sigma_{\rm Red}^{W} = \frac{\epsilon_0 r_{0b}^2}{2E_{\rm Red}} \ln\left\{1 + \exp\left[\frac{2\pi}{\epsilon_0}(E_{\rm Red} - V_{\rm Red})\right]\right\}, \qquad (1)$$

where $E_{\rm Red} = E_{\rm c.m.}/\xi$ is the reduced energy, $\epsilon_0 = \hbar\omega_0/\xi$ is the reduced barrier-curvature parameter, $r_{0b} = R_0/\eta^{(1/2)}$ is the reduced radius, $V_{\rm Red} = V_0/\xi$ is the reduced barrier height, and $\sigma_{\rm Red}^{W} = \sigma^{W}/\eta$ is the reduced cross section corresponding to Wong's formula. The parameter r_e originally used in Ref. [18], used later in Ref. [2], and the ratio $\hbar\omega_0/V_0$ used in the latter reference, can easily be related to the parameters in Eq. (1): $r_e = 1.44/V_{\rm Red}$, $\hbar\omega_0/V_0 = \epsilon_0/V_{\rm Red}$. All parameter values given in this Rapid Communication correspond to using units of MeV and femtometers for energies and distances, respectively.

Notice that a given set of values for r_{0b}, $V_{\rm Red}$, and ϵ_0 actually does determine a family of systems [i.e., those systems whose reaction cross sections fall on the corresponding curve of Eq. (1) when plotted in terms of reduced variables]. The actual barrier parameters for different members of a family are related to each other through the definition of the corresponding reduced parameters. The findings of Refs. [1,2] can then be rephrased by saying that, as far as total reaction cross sections are concerned, nuclear systems seem to group in different families, depending on the nature of the projectile: strongly bound, normal weakly bound, or halo projectiles.

The solid curve in Fig. 1 is the Wong-model fit obtained previously [2] for halo nuclei ($r_{0b} = 1.79$, $r_e = 1.83$, and $\hbar\omega_0/V_0 = 0.62$). This corresponds to reduced parameter values $V_{\rm Red} = 0.79$ and $\epsilon_0 = 0.49$. Only the experimental

*eli.aguilera@inin.gob.mx

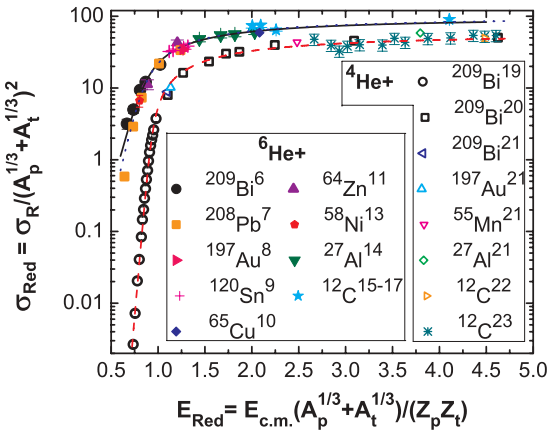

FIG. 1. (Color online) Reduced total reaction cross sections for different systems with ^{6}He and ^{4}He projectiles. References are given as right-hand-side superscripts of target symbols.

points for ^{6}He on targets of ^{27}Al, ^{64}Zn, and ^{209}Bi were considered in that fit. It is interesting to see that the data for all the additional systems with the ^{6}He projectile still follow the same trajectory, especially considering that the reduced-energy range has essentially been doubled. This further confirms that the family of systems with halo projectiles is well defined for the case of ^{6}He. We emphasize that this is true independently of the goodness of the model fit (i.e., the data clearly follow a well-defined trend, regardless of the model curve).

However, it is also interesting to try to interpret the data in terms of Wong's model because the involved parameters have a well-defined physical meaning. The fit of Eq. (1) to the whole ^{6}He data set gives the parameter values shown in the first line of Table I. It is worth mentioning that three experimental points account for ∼50% of the χ^2/N value, so the corresponding error bars may be underestimated. With this in mind, by considering the large number of independent experiments involved in producing the data, and by taking the simplicity of Wong's model into account, the obtained value of χ^2/N seems quite reasonable. The corresponding curve, shown with a dotted line in Fig. 1, is practically indistinguishable from the solid curve, except maybe at the very lowest energies.

In a fit such as this, where many different systems are involved, which span a wide energy range, one may expect that the extracted values for the barrier parameters should have a rather global character. These parameter values could, in principle, be extracted from measurements for one single system in the family, but a very large energy interval needs to be measured to get reliable results. This clearly has not been performed for ^{6}He projectiles. The global fit obtained here, by using reduced variables, should help minimize possible ambiguities in the reduced parameters, thus making the results quite reliable. This fit also has the additional bonus that data from many independent works, which use varied experimental techniques, are being utilized. As mentioned earlier, the particular parameter values for each system can then be calculated easily from the reduced ones.

TABLE I. Reduced Wong-model parameters for each projectile and respective values of χ^2 per degree of freedom. Variation of one parameter by the reported error will produce an approximately one unit increase in χ^2/N. N_{pts} is the number of points.

Projectile	V_{Red}	r_{0b}	ϵ_0	N_{pts}	χ^2/N
^{6}He	0.780 ± 0.014	1.79 ± 0.04	0.43 ± 0.06	28	4.3
^{4}He	0.913 ± 0.005	1.39 ± 0.05	0.175 ± 0.006	43	3.4

Figure 1 additionally includes reduced reaction cross sections for ^{4}He projectiles on a number of targets, essentially covering the same wide range of reduced energies as for ^{6}He, $0.7 \leqslant E_{Red} \leqslant 4.6$. The data were taken from Refs. [19–23], as indicated in the figure. The corresponding points also belong to one single family, which, in this case, can be characterized by a reduced Wong curve (dashed line) with parameter values given in the second line of Table I. In this case, 3 out of the 43 experimental points account for more than 50% of the χ^2/N value. With respect to this curve, a striking enhancement of the halo systems can be observed. This kind of enhancement was first noticed in Ref. [1]. From Table I, one can see that $V_{Red} \times r_{0b} \sim 1.4$ for ^{6}He and ∼1.3 for ^{4}He. By using the definition of the reduced parameters, it can be seen that these relations are similar to the well-known formula for the Coulomb potential V_C (MeV) of two point charges Z_pe, Z_te (e stands for the elementary charge), separated by R_0 (fm), $V_C = 1.44 Z_p Z_t / R_0$.

So, although the radius parameter is 30% larger for the halo projectile, the combined variation of the fitting parameters r_{0b} and V_{Red} from one curve to the other nearly follows the expected behavior for Coulomb barriers. However, since an $A^{1/3}$ scaling of the respective nuclear radii is already included in the reduced variables, it is clear that the barrier associated with ^{6}He reactions corresponds to a distance considerably larger than expected from the simple $A^{1/3}$ dependence. Then, this can be interpreted as a static halo effect directly related to the extended size of the halo nucleus. A similar size effect of the ^{6}He isotope on some measured reaction cross sections was discovered in the pioneering experiments of Tanihata *et al.* [24,25], which were performed in an energy regime much higher than the one analyzed in this Rapid Communication. Then, it seems that this size effect is somehow carried down to the lower-energy region involved in the data of Fig. 1. According to the r_{0b}^2 factor in Wong's formula, Eq. (1), this effect should be present for all energies.

The large difference in the ϵ_0 values for the two projectiles (see Table I) can be interpreted as an additional halo effect influencing the ^{6}He data. It implies an exceptionally large barrier curvature (exceptionally narrow barrier) for the halo systems. In Ref. [2], it was noticed that this corresponds to an increased diffuseness of the absorption in ℓ space, most probably caused by the enhanced transfer/breakup cross sections observed for these projectiles. Consistent with these observations, this apparently dynamic effect is important mainly in the enery region near and below the barrier. For larger energies, the influence of the two appearances of ϵ_0 in Eq. (1) tend to cancel each other; as a matter of fact, in the case of relatively large energies, the equation reduces to $\sigma_{Red}^W = \pi r_{0b}^2 (1 - V_{Red}/E_{Red})$, which gives a well-known formula when the reduced variables are converted back to normal quantities. Around the barrier, the s-wave contribution to the cross section

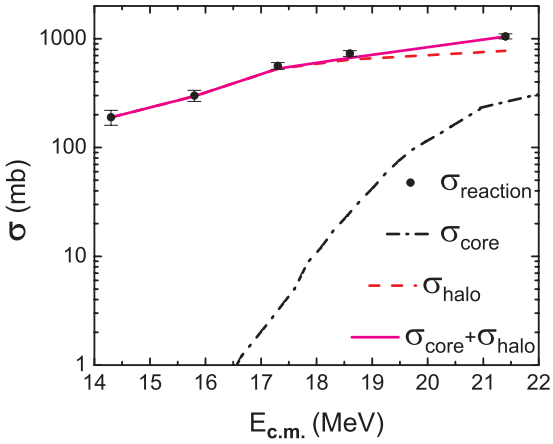

FIG. 2. (Color online) Total reaction and transfer/breakup (halo) cross sections for ^{6}He + ^{209}Bi (taken from Ref. [3]).

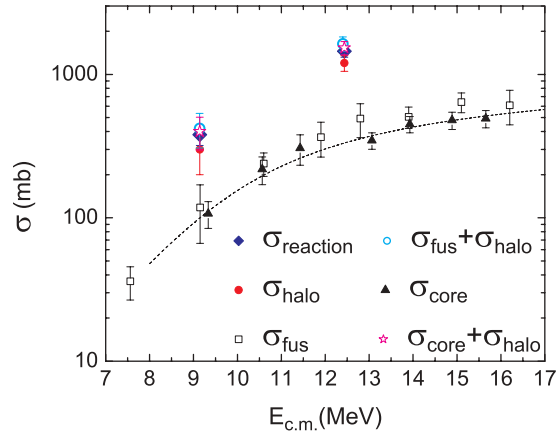

FIG. 3. (Color online) Total reaction, transfer/breakup (halo), and fusion cross sections for ^{6}He + ^{64}Zn (data from Refs. [11,12]).

dominates, and the approximation $\hbar\omega_\ell \approx \hbar\omega_0$ should work well, no matter how large $\hbar\omega_0$ might be. This is needed to assess the validity of Wong's formula [18].

Under the assumption of core-halo decoupling for the halo nucleus ^{6}He, the difference between the solid and the dashed curves in Fig. 1 should be caused by the reactions with the two-neutron halo. The reactions of ^{6}He with a ^{209}Bi target at energies close to the Coulomb barrier [4–6] were analyzed within this context in Ref. [3]. The transfer/breakup processes represent the possible reactions with the $2n$ halo, indicated by the $\sigma_{\rm halo}$ curve in Fig. 2. The sum of fusion and transfer/breakup cross sections, which represents the total reaction cross section, is displayed with solid circles in the figure. As for the reactions with the α core, the corresponding cross sections [19,20] were multiplied times $\eta(^{6}\mathrm{He} + ^{209}\mathrm{Bi})/\eta(^{4}\mathrm{He} + ^{209}\mathrm{Bi})$ and the respective energies were multiplied times $\xi(^{6}\mathrm{He} + ^{209}\mathrm{Bi})/\xi(^{4}\mathrm{He} + ^{209}\mathrm{Bi})$ to obtain the $\sigma_{\rm core}$ curve in Fig. 2. This figure shows that the $\sigma_{\rm core} + \sigma_{\rm halo}$ curve reproduces the total reaction data quite well, consistent with a decoupling core halo. Here, our purpose is to investigate whether such a decoupling is also present in reactions of ^{6}He with other targets. There is only one more system where, in addition to the total reaction cross sections, all relevant reactions associated with the neutron halo have also been measured. This is the ^{6}He + ^{64}Zn system, which we analyze now.

For the ^{6}He + ^{64}Zn system, angular distributions for elastic scattering and transfer/breakup processes were measured, at two near-Coulomb barrier energies, by Di Pietro *et al.* [11]. An optical model analysis of the elastic scattering data gave total reaction cross sections of 380 ± 60 and 1450 ± 130 mb at $E_{\rm c.m.} = 9.1$ and 12.4 MeV, respectively. The points indicated as $\sigma_{\rm reaction}$ in Fig. 3 represent these values. The integrated transfer/breakup cross sections for the same energies were reported as 300 ± 100 and 1200 ± 150 mb, respectively. These values account for the reactions with the halo and, thus, are indicated as $\sigma_{\rm halo}$ in the figure.

Fusion excitation functions for ^{4,6}He + ^{64}Zn were also measured in Ref. [11] and later extended to higher energies by the same group [12]. For the ^{6}He projectile, the whole measured excitation function is represented by the $\sigma_{\rm fus}$ points in Fig. 3. The sum of $\sigma_{\rm fus}$ with the transfer/breakup cross section ($\sigma_{\rm halo}$) is seen to be consistent with $\sigma_{\rm reaction}$ at the two energies where data exist for the last two quantities (a simple interpolation was performed to estimate $\sigma_{\rm fus}$ at 12.4 MeV). The fact that fusion plus transfer/breakup processes do actually saturate the total reaction cross section at near-Coulomb barrier energies was also observed in the previous data for the ^{6}He + ^{209}Bi system [3,6].

For the present system, the reactions with the core can be deduced from the fusion data for ^{4}He + ^{64}Zn, just by performing an appropriate scaling [3]. The results of such a scaling are shown as $\sigma_{\rm core}$ in Fig. 3. The dashed curve represents a Wong-model fit [18] to the corresponding points ($\chi^2/N = 0.3$). Because $\sigma_{\rm fus}$ and $\sigma_{\rm core}$ are consistent with each other within error bars, from the observations of the last paragraph, it is clear that $\sigma_{\rm core} + \sigma_{\rm halo}$ should, in turn, be consistent with $\sigma_{\rm reaction}$. The star points in Fig. 3 corroborate this fact. The values of $\sigma_{\rm core}$ at the two energies where $\sigma_{\rm halo}$ was measured were estimated from the dashed curve in the figure by keeping the error bar of the closest measured point. Then, we conclude that the data for ^{4,6}He + ^{64}Zn are consistent with a core-halo decoupling for ^{6}He.

To summarize, a systematic study of total reaction cross sections for ^{6}He and ^{4}He projectiles has been performed. A comparison between these two projectiles is interesting because ^{4}He is the core of the halo nucleus ^{6}He. An appropriate reduction of energies and cross sections plays a key role in allowing a comparison of data for different systems. All reduced cross sections for ^{6}He projectiles fall on the same trajectory when plotted versus the respective reduced energy. A variation of Wong's formula, where absolute quantities are replaced by reduced ones, allows one to nicely characterize the trajectory in terms of reduced barrier parameters. The large number of systems fitted, which covers a wide energy range, should make the extracted parameters quite reliable.

The points corresponding to ^{4}He projectiles also follow a well-defined trajectory that, as expected, lies below the one for ^{6}He and can be characterized by a different Wong-type curve. The difference between the two trajectories can be ascribed to the halo character of ^{6}He, which, in this interpretation, produces two separate effects. One is a geometric effect,

related to the extended size of the halo nucleus, which affects the cross sections in the whole energy region. The other effect is important mainly in the energy region near or below the barrier. It seems to have a dynamic origin, and it is probably related to the enhanced transfer/breakup processes that have been observed for ^{6}He. This effect is accounted for in the Wong model by an unusually narrow barrier.

Static effects of the halo are equivalent for all targets studied, no matter how light or heavy they are. The kinematic regime below $V_{\mathrm{Red}} = 0.78$, where dynamic effects may be important, needs to be studied for more systems with the ^{6}He projectile to elucidate possible nuclear structure effects.

Evidence was also presented, which indicates that a core-halo decoupling is present for the neutron-halo nucleus ^{6}He in reactions with ^{64}Zn. As shown in a previous work, this is also true for reactions with ^{209}Bi, so the decoupling seems to be independent of the target. The previous conclusions are based upon comparison of purely experimental data for both the nucleus and its core. The present results give further support to the hypothesis that such a decoupling is actually a characteristic feature of true halo systems.

E.F.A. wishes to acknowledge the warm hospitality of all personnel at the Universidad de Huelva. This work has been partially supported by the CONACYT (México), by the "XV Plan Propio de Investigación" from the Universidad de Huelva, and by the Spanish Ministry of Science under Contract No. FPA2007-63074.

[1] E. F. Aguilera *et al.*, Phys. Rev. C **79**, 021601(R) (2009).
[2] J. J. Kolata and E. F. Aguilera, Phys. Rev. C **79**, 027603 (2009).
[3] E. F. Aguilera, J. J. Kolata, and L. Acosta, Phys. Rev. C **81**, 011604(R) (2010).
[4] J. J. Kolata *et al.*, Phys. Rev. Lett. **81**, 4580 (1998).
[5] E. F. Aguilera *et al.*, Phys. Rev. Lett. **84**, 5058 (2000).
[6] E. F. Aguilera *et al.*, Phys. Rev. C **63**, 061603(R) (2001).
[7] A. M. Sánchez-Benítez *et al.*, Nucl. Phys. A **803**, 30 (2008).
[8] O. R. Kakuee *et al.*, Nucl. Phys. A **765**, 294 (2006).
[9] P. N. de Faria *et al.*, Phys. Rev. C **81**, 044605 (2010).
[10] A. Chatterjee *et al.*, Phys. Rev. Lett. **101**, 032701 (2008).
[11] A. Di Pietro *et al.*, Phys. Rev. C **69**, 044613 (2004).
[12] A. Di Pietro *et al.*, Phys. At. Nucl. **69**, 1366 (2006).
[13] L. R. Gasques *et al.*, Phys. Rev. C **67**, 024602 (2003); L. R. Gasques (private communication).
[14] E. A. Benjamim *et al.*, Phys. Lett. B **647**, 30 (2007).
[15] R. J. Smith, J. J. Kolata, K. Lamkin, A. Morsad, K. Ashktorab, F. D. Becchetti, J. A. Brown, J. W. Janecke, W. Z. Liu, and D. A. Roberts, Phys. Rev. C **43**, 761 (1991).
[16] M. Milin *et al.*, Nucl. Phys. A **730**, 285 (2004).
[17] R. E. Warner *et al.*, Phys. Rev. C **51**, 178 (1995).
[18] C. Y. Wong, Phys. Rev. Lett. **31**, 766 (1973).
[19] A. R. Barnett and J. S. Lilley, Phys. Rev. C **9**, 2010 (1974).
[20] P. Singh, A. Chatterjee, S. K. Gupta, and S. S. Kerekatte, Phys. Rev. C **43**, 1867 (1991).
[21] L. McFadden and G. R. Satchler, Nucl. Phys. **84**, 177 (1966).
[22] M. E. Farid, Z. M. M. Mahmoud, and G. S. Hassan, Phys. Rev. C **64**, 014310 (2001).
[23] E. B. Carter, G. E. Mitchell, and R. H. Davis, Phys. Rev. **133**, B1421 (1964).
[24] I. Tanihata *et al.*, Phys. Lett. B **160**, 380 (1985).
[25] I. Tanihata, H. Hamagaki, O. Hashimoto, Y. Shida, N. Yoshikawa, K. Sugimoto, O. Yamakawa, T. Kobayashi, and N. Takahashi, Phys. Rev. Lett. **55**, 2676 (1985).